

Photo-Induced and Resist-Free Imprint Patterning of Fullerene Materials for Use in Functional Electronics

Andrzej Dzwilewski, Thomas Wågberg, and Ludvig Edman*

The Organic Photonics and Electronics Group, Department of Physics, Umeå University, SE-901 87 Umeå, Sweden

Received October 15, 2008; E-mail: ludvig.edman@physics.umu.se

Ⓜ This paper contains enhanced objects available on the Internet at <http://pubs.acs.org/jacs>.

Abstract: We report a novel and potentially generic method for the efficient patterning of films of organic semiconductors and demonstrate the merit of the method on the high-solubility fullerene [6,6]-phenyl C₆₁-butyric acid methyl ester (PCBM). The patterning technique is notably straightforward as it requires no photoresist material and encompasses only two steps: (i) exposure of select film areas to visible laser light during which the PCBM monomer is photochemically converted into a dimeric state, and (ii) development via solvent washing after which the nonexposed portions of the PCBM film are selectively removed. Importantly, the method is highly benign in that it leaves the electronic properties of the remaining patterned material intact, which is directly evidenced by the fact that we fabricate fully functional arrays of micrometer-sized field-effect transistors with patterned PCBM as the active material.

I. Introduction

The combined opportunity for solution processing and easy patterning of organic materials with desirable electronic properties (e.g., high electronic mobility and efficient fluorescence) is a key attribute, which makes the field of organic electronics very attractive for emerging applications. A range of patterning techniques—spanning from subtractive lithography,^{1–3} over chemical and electrochemical deactivation of electronic function in select areas,^{4,5} to additive stamping and printing^{6–9}—has been demonstrated. However, organic electronic materials can be rather fragile, and the performance of devices based on such materials is often adversely affected by the conventional use of reactive chemicals and/or UV light during subtractive patterning and deactivation processes (with a few notable exceptions)^{1,2} as well as by the less-than-ideal film morphology that typically results from printing. Thus, it is relevant to develop gentle and straightforward patterning techniques of high-quality solution-processed films, which leave the electronic properties of the remaining patterned organic material uncompromised. Here, we introduce a photoinduced and resist-free imprinting (PRI)

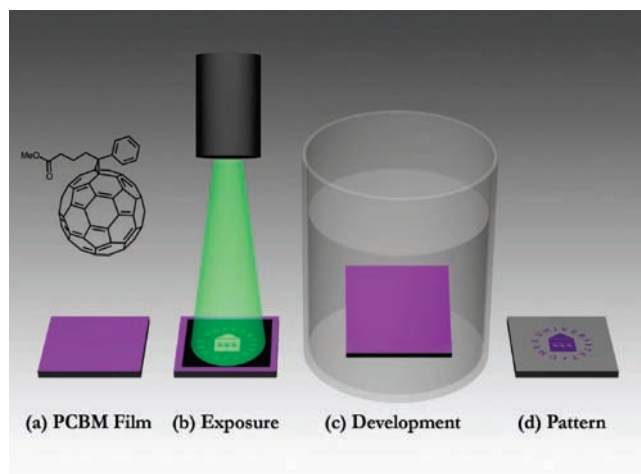


Figure 1. Schematic illustrating the process flow diagram for one representation of the PRI patterning of a PCBM film. (a) Solution-processed PCBM film on a substrate. (b) Laser-light exposure of the film through a (black) shadow mask, which transforms the exposed PCBM molecules into a low-solubility (dimeric) state. (c) Solution development of the exposed PCBM film, which selectively removes the nonexposed portions of the film. (d) Resulting pattern of electronically active PCBM.

method, which comprises only two steps (as presented in Figure 1): (i) laser-light exposure during which a desired pattern is directly imprinted into the organic material, and (ii) solution development during which the nonexposed portions of the material are selectively removed. We demonstrate the functionality of the PRI technique on various types of solution-deposited [6,6]-phenyl C₆₁-butyric acid methyl ester (PCBM) films, which are of interest for, for example, solar cell^{10–13} and transistor^{14–20} applications. Importantly, we show that the PRI technique is compatible with simultaneous benign and high-resolution patterning, as evidenced by that field-effect transistors comprising

- (1) DeFranco, J. A.; Schmidt, B. S.; Lipson, M.; Malliaras, G. G. *Org. Electron.* **2006**, *7*, 22.
- (2) Huang, J.; Xia, R.; Kim, Y.; Wang, X.; Dane, J.; Hofmann, O.; Mosley, A.; de Mello, A. J.; de Mello, J. C.; Bradley, D. D. C. *J. Mater. Chem.* **2007**, *17*, 1043.
- (3) Balocco, C.; Majewski, L. A.; Song, A. M. *Org. Electron.* **2006**, *7*, 500.
- (4) Yoshioka, Y.; Calvert, P. D.; Jabbour, G. E. *Macromol. Rapid Commun.* **2005**, *26*, 238.
- (5) Tehrani, P.; Kanciurowska, A.; Crispin, X.; Robinson, N. D.; Fahlman, M.; Berggren, M. *Solid State Ionics* **2007**, *177*, 3521.
- (6) Xia, Y.; Whitesides, G. M. *Annu. Rev. Mater. Sci.* **1998**, *28*, 153.
- (7) Sirringhaus, H.; Kawase, T.; Friend, R. H.; Shimoda, T.; Inbasekaran, M.; Wu, W.; Woo, E. P. *Science* **2000**, *290*, 2123.
- (8) Pardo, D. A.; Jabbour, G. E.; Peyghambarian, N. *Adv. Mater.* **2000**, *12*, 1249.
- (9) Zhang, F.; Nyberg, T.; Inganäs, O. *Nano Lett.* **2002**, *2*, 1373.

micrometer-sized patterned PCBM as the active material are fully functional.

II. Experimental Methods

PCBM (Solenne, $\geq 99.5\%$) was dissolved in chlorobenzene (Aldrich, anhydrous 99.8%). Highly p-doped Si (the gate electrode) with a 200 nm layer of SiO₂ (the gate dielectric) was used as substrates. Drop-cast PCBM films were fabricated by deposition of two drops of a 10 mg/mL solution, with a 1 min time interval, onto a substrate maintained at $T = 400$ K. The films were thereafter dried at $T = 400$ K for 5 min. We selected to employ the “double-drop” casting process onto heated substrates in order to attain optimum transistor performance and repeatability. A similar technique was employed by Anthopoulos et al.¹⁶ The spin-cast films were fabricated by spin casting a 20 mg/ml solution at 800 rpm.

The exposure of drop-cast PCBM films was performed with an Ar-ion laser ($\lambda = 488$ nm, ~ 5 mW/mm² at the PCBM film surface) for 1 h, and the development was performed by rinsing with a binary “developer solution” comprising chloroform and acetone (3:1 volume ratio). The patterned film was dried at $T = 400$ K for 2 min. The exposure of the spin-cast films was performed with a green laser ($\lambda = 532$ nm, ~ 20 mW/mm²) for 15 min. The development was performed by immersion the film in a chloroform:acetone (1:3 volume ratio) developer solution for 1 min. The patterned film was dried at $T = 373$ K for 3 min. The possibility for effective exposure of PCBM films with a range of laser wavelengths (here $\lambda = 488$ nm and $\lambda = 532$ nm) is a direct reflection of the broad absorption spectrum of PCBM. Moreover, the absorption coefficient of PCBM at $\lambda \approx 500$ nm is $\sim 10^4$ cm⁻¹,¹⁷ which demonstrates that the laser excitation intensity throughout the herein employed PCBM films with a thickness of ~ 100 nm is relatively uniform.

The laser beam is made to diverge in the experiments (as depicted in the schematic in Figure 1) since a negative lens is placed right after the laser. The introduction of this lens allowed us to control the diameter of the laser beam incident on the PCBM film. The original beam emerging from the laser had a diameter of 0.8 mm, but the incident beam on the PCBM film ranged between 0.2 and 1 cm in different experiments.

Au source and drain electrodes (thickness = 100 nm) were fabricated by thermal evaporation, using a shadow mask to define the electrode structures. The electrodes were positioned in a bottom-contact configuration for the drop-cast devices ($W = 1.2$ mm, $L = 110$ μ m), and in a top-contact configuration for the spin-cast devices ($W = 1.2$ mm, $L = 110$ μ m). All device handling were carried out under inert atmosphere in two interconnected Ar-filled glove boxes (O₂, H₂O < 1 ppm) and an integrated thermal evaporation unit.

The FET characterization was performed using a Keithley 4200 semiconductor characterization system, with the source electrode grounded. In total, we have fabricated and patterned ~ 100 devices for each of the presented deposition techniques. We find that $\sim 90\%$ of the FETs with drop-cast PCBM as the active material are functional after patterning, and that the nearly 100% of the spin-cast PCBM FETs are functional at the end of the patterning process.

Raman measurements were performed under Ar atmosphere with a Renishaw Raman 1000 spectrometer equipped with a diode laser ($\lambda = 780$ nm, < 20 mW/cm²) and with a resolution of 1 cm⁻¹. 80 nm thick C₆₀ films were produced by thermal evaporation. The polymerization of the C₆₀ films was performed with a He-Ne laser ($\lambda = 633$ nm, ~ 5 mW/mm²).

III. Results and Discussion

It has been demonstrated that the low-solubility fullerene C₆₀ can form various polymeric phases during exposure to visible laser light.^{18,23} The basic mechanism behind the formation of chemically connected C₆₀ structures is that intramolecular *sp*² (double) bonds are activated by the laser exposure, and that two such activated bonds on neighboring C₆₀ molecules in an appropriate configuration form a chemical connection via two intermolecular *sp*³ (single) bonds. The photoinduced polymerization process of C₆₀ can be conveniently resolved with Raman spectroscopy, since the strongest Raman-active vibrational mode in C₆₀—the A_g(2) mode—is very sensitive to the electron density at the intramolecular double bonds, and the formation of intermolecular bonds between C₆₀ molecules lowers the electron density at the intramolecular double bonds. It has been shown that the A_g(2) mode downshifts with approximately 5 cm⁻¹/intermolecular bond/C₆₀ molecule, such that it is positioned at 1468 cm⁻¹ in “free” C₆₀ molecules,^{24–29} at 1464 cm⁻¹ in dimers with one intermolecular bond per C₆₀ molecule,^{24,25} at 1459 cm⁻¹ in linear polymers with two intermolecular bonds per C₆₀ molecule,^{24–26} and at 1454 cm⁻¹ in a branched polymer sample with three intermolecular bonds per C₆₀ molecule.²⁹

PCBM chemically differs from C₆₀ in that it has a side group grafted onto the electroactive C₆₀ molecule (see top part of Figure 1a). The side group brings the desired advantages that PCBM, in contrast to C₆₀, is highly soluble in common organic solvents, and that it accordingly is possible to fabricate high-quality PCBM films directly from solution. For the same reason—the added side group—it was reasonable to anticipate that it would be impossible to attain an appropriate configuration of two activated PCBM molecules in close proximity that is prone to form intermolecular chemical bonds.

Figure 2a presents Raman spectra recorded on a pristine C₆₀ film (top trace), a laser-exposed C₆₀ film (second trace from

- (10) Brabec, C. J.; Sariciftci, N. S.; Hummelen, J. C. *Adv. Funct. Mater.* **2001**, *11*, 15.
- (11) Dennler, G.; Prall, H. J.; Koeppel, R.; Egginger, M.; Autengruber, R.; Sariciftci, N. S. *Appl. Phys. Lett.* **2006**, *89*, 073502.
- (12) Offermans, T.; Meskers, S. C. J.; Janssen, R. A. J. *Org. Electron.* **2007**, *8*, 325.
- (13) Kim, J. Y.; Lee, K.; Coates, N. E.; Moses, D.; Nguyen, T. Q.; Dante, M.; Heeger, A. J. *Science* **2007**, *317*, 222.
- (14) Waldauf, C.; Schilinsky, P.; Perisutti, M.; Hauch, J.; Brabec, C. J. *Adv. Mater.* **2003**, *15*, 2084.
- (15) Haddock, J. N.; Zhang, X. H.; Domercq, B.; Kippelen, B. *Org. Electron.* **2005**, *6*, 182.
- (16) Anthopoulos, T. D.; Kooistra, F. B.; Wondereg, H. J.; Kronholm, D.; Hummelen, J. C.; de Leeuw, D. M. *Adv. Mater.* **2006**, *18*, 1679.
- (17) Hoppe, H.; Arnold, N.; Sariciftci, N. S.; Meissner, D. *Sol. Energy Sol. Cells* **2003**, *80*, 105.
- (18) Dzwilewski, A.; Wågberg, T.; Edman, L. *Phys. Rev. B* **2007**, *75*, 075203.
- (19) Singh, T. B.; Marjanovic, N.; Stadler, P.; Auinger, M.; Matt, G. J.; Gunes, S.; Sariciftci, N. S.; Schwodiauer, R.; Bauer, S. *J. Appl. Phys.* **2005**, *97*, 083714.
- (20) Dodabalapur, A.; Katz, H. E.; Torsi, L.; Haddon, R. C. *Appl. Phys. Lett.* **1996**, *68*, 1108.

- (21) Anthopoulos, T. D.; Tanase, C.; Setayesh, S.; Meijer, E. J.; Hummelen, J. C.; Blom, P. W. M.; de Leeuw, D. M. *Adv. Mater.* **2004**, *16*, 2174.
- (22) Dimitrakopoulos, C. D.; Malenfant, P. R. L. *Adv. Mater.* **2002**, *14*, 99.
- (23) Rao, A. M.; Zhou, P.; Wang, K. A.; Hager, G. T.; Holden, J. M.; Wang, Y.; Lee, W. T.; Bi, X. X.; Eklund, P. C.; Cornett, D.S.; Duncan, M. A.; Amster, I. J. *Science* **1993**, *259*, 955.
- (24) Burger, B.; Winter, J.; Kuzmany, H. *Z. Phys. B: Condens. Matter* **1996**, *101*, 227.
- (25) Lebedkin, S.; Gromov, A.; Giesa, S.; Gleiter, R.; Renker, B.; Rietschel, H.; Kratschmer, W. *Chem. Phys. Lett.* **1998**, *285*, 210.
- (26) Eklund, P. C.; Zhou, P.; Wang, K. A.; Dresselhaus, G.; Dresselhaus, M. S. *J. Phys. Chem. Solids* **1992**, *53*, 1391.
- (27) Edman, L.; Ferry, A.; Jacobsson, P. *Macromolecules* **1999**, *32*, 4130.
- (28) Kovács, É.; Oszlányi, G.; Pekker, S. *J. Phys. Chem. B* **2005**, *109*, 11913.
- (29) Karachevtsev, V. A.; Mateichenko, P. V.; Nedbailo, N. Y.; Peschanskii, A. V.; Plokhotichenko, A. M.; Vovk, O. M.; Zubarev, E. N.; Rao, A. M. *Carbon* **2004**, *42*, 2091.

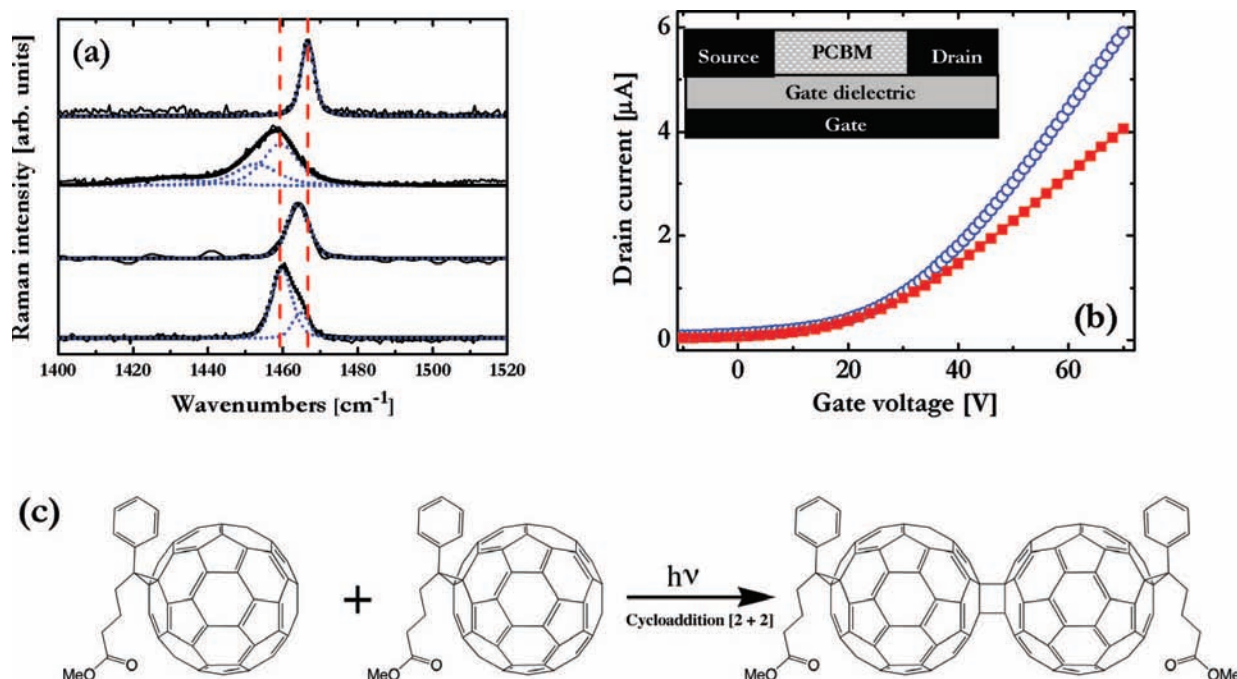


Figure 2. (a) Raman spectra of a pristine C₆₀ film (top trace), a laser-exposed C₆₀ film (second trace from top), a pristine PCBM film (second trace from bottom), and a laser-exposed PCBM film (bottom trace). The vertical dashed lines are a guide-to-the-eye; the line to the right represents the position of the Ag(2) mode in nonpolymerized C₆₀, and the line to the left represents the position of the Ag(2) mode in linearly polymerized C₆₀. (b) Transfer characteristics of a PCBM FET, measured at a drain voltage of V_D = +60 V, before (○) and after (■) the PCBM active material was exposed to an Ar-ion laser. (Inset) Schematic of the FET structure. (c) Proposed reaction where two PCBM molecules are photoactivated by the exposure to visible laser light, and subsequently form a dimeric PCBM structure.

top), a pristine PCBM film (second trace from bottom), and a laser-exposed PCBM film (bottom trace). The different components of the spectra (indicated by dotted lines) were deconvoluted by fitting with Voigtian line shapes. From the assignment provided in the previous paragraphs, it is clear that the laser exposure has transformed “free” C₆₀ molecules (A_g(2) mode at 1468 cm⁻¹ in top trace) into a fully polymerized structure, with linearly polymerized C₆₀ as the major component (dominant A_g(2) mode at 1459 cm⁻¹ in second trace from top).

Very few Raman studies have been published on PCBM,³⁰ and we have not been able to find any data with reasonable resolution for the A_g(2) mode. We find that the A_g(2) mode is located at 1465 cm⁻¹ in pristine PCBM (second trace from bottom), which is consistent with the previous assignment considering that “free” PCBM molecules are reminiscent to C₆₀ dimers in that both species contain one “intermolecular” bond per C₆₀ molecule. The Raman data for the laser-exposed PCBM film are interesting. The major A_g(2) mode is positioned at 1460 cm⁻¹, with a minor component at 1465 cm⁻¹. This implies that a minor fraction of the PCBM molecules in the laser-exposed film remains “free”, but, more importantly, that a significant majority of the PCBM molecules has formed chemical structures comprising one new intermolecular bond as compared to “free” PCBM. We also note that it has been reported that PCBM crystallizes into a structure in which the shortest center-to-center distance is less than in C₆₀.³¹ With this information at hand, we draw the conclusion that the laser exposure has transformed “free” PCBM molecules into a dimeric structure, as outlined in Figure 2c. The fact that the laser exposure causes PCBM to

end up in a dimeric configuration, while C₆₀ frequently continues to form intermolecular bonds to end up in a polymeric configuration, can be rationalized with that the side group of PCBM effectively shields parts of the molecule from chemical reactions and effectively hinders PCBM dimers from forming longer oligomeric and polymeric structures. We have initiated complementary NMR and mass spectrometry studies in order to establish the exact configuration of the PCBM dimers within the laser-exposed PCBM film, and we hope to be able to come back with detailed information on the structure of the laser-exposed PCBM molecules in a future publication.

We have fabricated field effect transistors (FETs) with PCBM as the active material (see inset in Figure 2b for a schematic device structure) to establish the effect of the dimerization process on the electronic mobility of PCBM. Figure 2b shows the transfer characteristics of a pristine-PCBM FET (○) and the same FET after the PCBM active material had been dimerized via exposure to laser light (■). We calculate the electron mobility (μ_n) and the threshold voltage (V_T) by fitting the conventionally employed FET equation:

$$I_d^{0.5} = \left(\frac{WC\mu_n}{2L} \right)^{0.5} * (V_G - V_T) \quad (1)$$

to our transfer characteristics data in the saturation regime. I_d, W, C, L, and V_G represent the drain current, the channel width, the device capacitance per unit area, the channel length, and the gate voltage, respectively. For PCBM monomers (i.e., before exposure) we find that μ_n = 0.016 cm²/Vs and V_T = 6 V, and for PCBM dimers (i.e., after exposure) we find that μ_n = 0.010 cm²/Vs and V_T = 0 V. These are typical values for our investigated devices, and we consistently find that the electron mobility and the threshold voltage decrease *slightly* after the

(30) Klimov, E.; Li, W.; Yang, X.; Hoffmann, G. G.; Loos, J. *Macromolecules* **2006**, *39*, 4493.

(31) Rispen, M. T.; Meetsma, A.; Rittberger, R.; Brabec, C. J.; Sariciftci, N. S.; Hummel, J. C. *Chem. Commun.* **2003**, *17*, 2116.

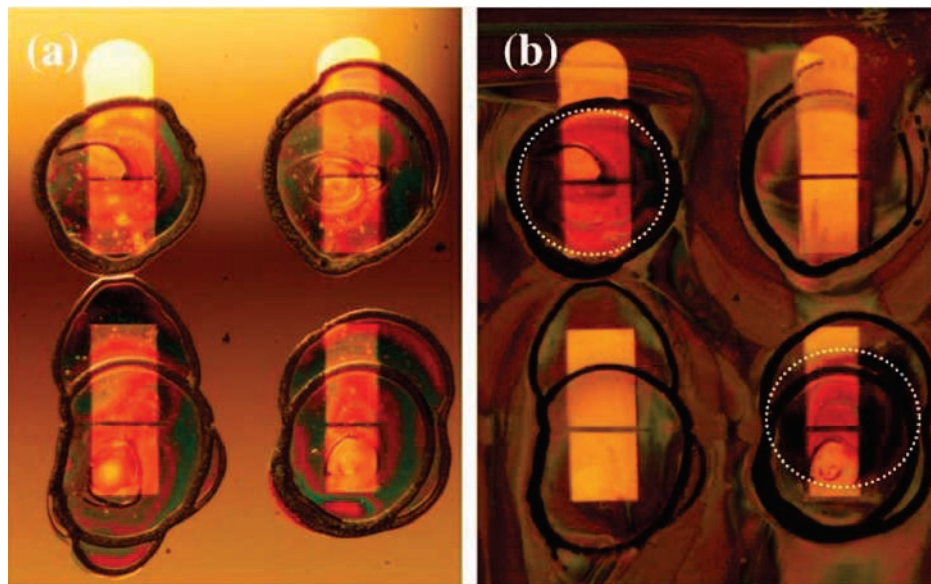


Figure 3. (a) Photograph of a 2×2 array of pristine-PCBM FETs on the same substrate. The FET structure consisted of Au electrodes in a bottom-contact configuration and a “double-drop” cast PCBM active material. (b) Photograph of the same array of FETs after the PCBM active material in the top-left and the bottom-right device had been exposed to visible laser light, and all four FETs thereafter had been separately rinsed with the developer solution. The dotted circles mark the positions at which the laser was exposing the PCBM material.

laser exposure, as was also the case for C_{60} FETs following laser-induced photopolymerization of the active material.¹⁸

A notably interesting and important result of the laser exposure of PCBM, and its transformation from “free” molecules into dimers, is that its solubility in common organic solvents changes drastically (in agreement with the behavior that has been reported for polymerized C_{60}).^{32,33} This observation, in combination with the demonstrated retained electronic mobility for dimerized PCBM, suggests that a novel photoinduced and resist-free imprinting (PRI) patterning of solution-processed and electronically active PCBM films is possible. Figure 3a shows a photograph of a substrate comprising four identically prepared pristine-PCBM FETs, with a “double-drop” cast PCBM film deposited on top of the source and drain electrodes as the active material. The dark and circular-shaped “edge lines” surrounding the transistor channels were formed at the outer circumferences of the drying PCBM solution drops during the deposition of the active material.

The PCBM active material in the top-left and bottom-right FETs was exposed to Ar-ion laser light with a spot diameter of ~ 2 mm for 1 h. Thereafter, the entire substrate was positioned at a 45° angle, and all FETs on the substrate developed by separate rinsing with ~ 1 mL of chloroform:acetone (3:1 by volume) developer solution extruded from a syringe. Figure 3b shows a photograph of the FET array taken after the entire exposure-development cycle. It demonstrates that the laser-exposed PCBM material (indicated by the dotted circles) is intact. This is in sharp contrast to the nonexposed PCBM material in the bottom-left device and top-right device (and outside the dotted circles in the other two devices), which is almost completely removed by the developer solution. The only significant traces of PCBM material that can be observed in

the nonexposed devices after development are located in the “edge lines”, which are positioned far off the active transistor channels. These “edge lines” are significantly thicker than the rest of the PCBM active material, and also, in some cases, exposed to minor scattered laser light during the exposure step, which rationalizes why they to some extent remain after the rinsing process.

We have measured the transistor characteristics for a large number of FETs, with the active PCBM material deposited by drop casting (see Figure 3). Figure 4 presents typical output characteristics (i.e., the drain current vs the drain voltage at different gate voltages) for two such FETs on the same substrate. Figure 4a shows the output data for a pristine-PCBM FET (device A), and Figure 4b shows the output data for the same FET after it had been developed by rinsing with the developer solution. The pristine-PCBM FET exhibits well-behaved transistor characteristics, while the response of the developed but nonexposed PCBM-FET is effectively zero (note the expanded y-axis scale). The latter is as expected considering that the nonexposed active material comprising “free” PCBM molecules is effectively removed from the FET channel region by the rinsing with the developer solution (see Figure 3).

It is then more interesting to establish the transistor characteristics at the different stages of the PRI patterning process applied to a PCBM-FET (device B located on the same substrate as device A). Figure 4c shows the output characteristics for the PCBM-FET in its pristine condition, Figure 4d shows the output data after the same FET had been exposed, and Figure 4e shows the output data after the exposed FET subsequently had been developed. We have employed eq 1 to calculate that a typical PCBM-FET exhibits an electron mobility of $\mu_n = 0.016$ cm^2/Vs in the pristine state, $\mu_n = 0$ cm^2/Vs after only development, $\mu_n = 0.010$ cm^2/Vs after only exposure, and $\mu_n = 0.006$ cm^2/Vs after exposure and subsequent development (i.e., patterning). The PRI-patterned PCBM-FETs consistently exhibit significant electron mobility and well-behaved output characteristics, with a linear increase in the drain current at low drain voltage

- (32) Hebard, A. F.; Eom, C. B.; Fleming, R. M.; Chabal, Y. J.; Muller, A. J.; Glarum, S. H.; Pietsch, G. J.; Haddon, R. C.; Mujsce, A. M.; Paczkowski, M. A.; Kochanski, G. P. *Appl. Phys. A: Mater. Sci. Process.* **1993**, *57*, 299.
 (33) McGinnis, S.; Norin, L.; Jansson, U.; Carlsson, J. O. *Appl. Phys. Lett.* **1997**, *70*, 586.

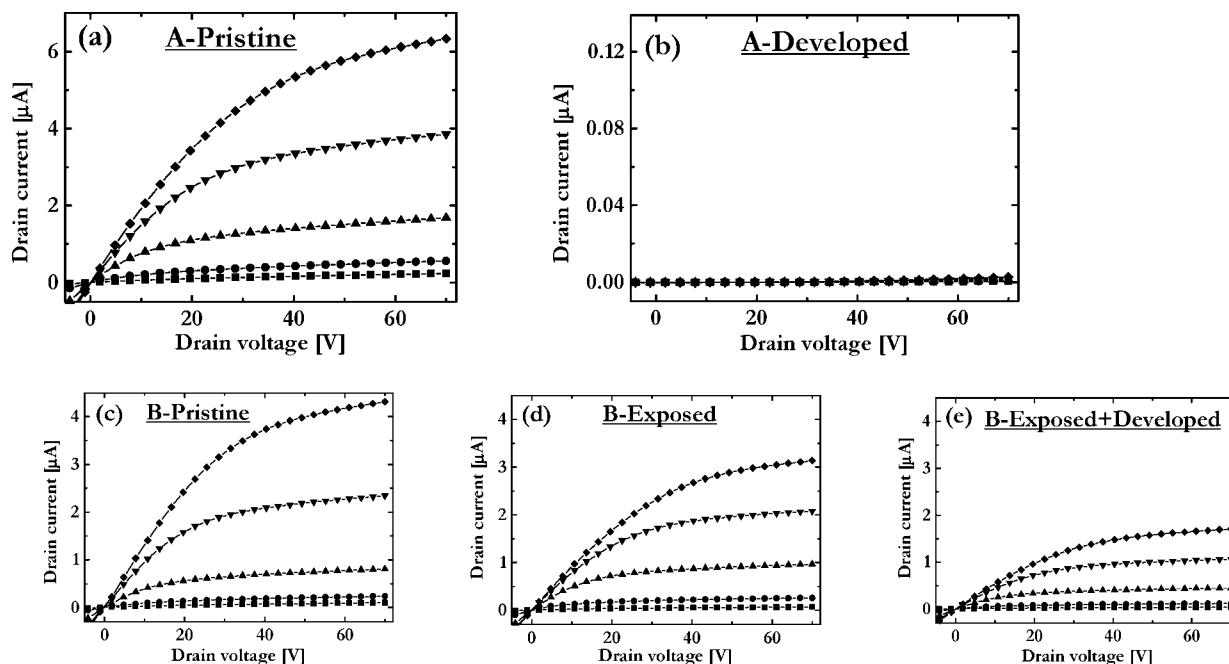


Figure 4. Output characteristics of two PCBM-FET devices termed “A” and “B” in an array on a substrate. (a) Device A in its pristine condition, and (b) after solely development with the developer solution (i.e., no exposure to laser light). (c) Device B in its pristine condition, (d) after laser-light exposure, and (e) after exposure and development. Note that the y-axis scale in (b) is expanded by a factor of 50. The gate voltage was increased in a sequential fashion from 0 V (squares) to 75 V (diamonds).

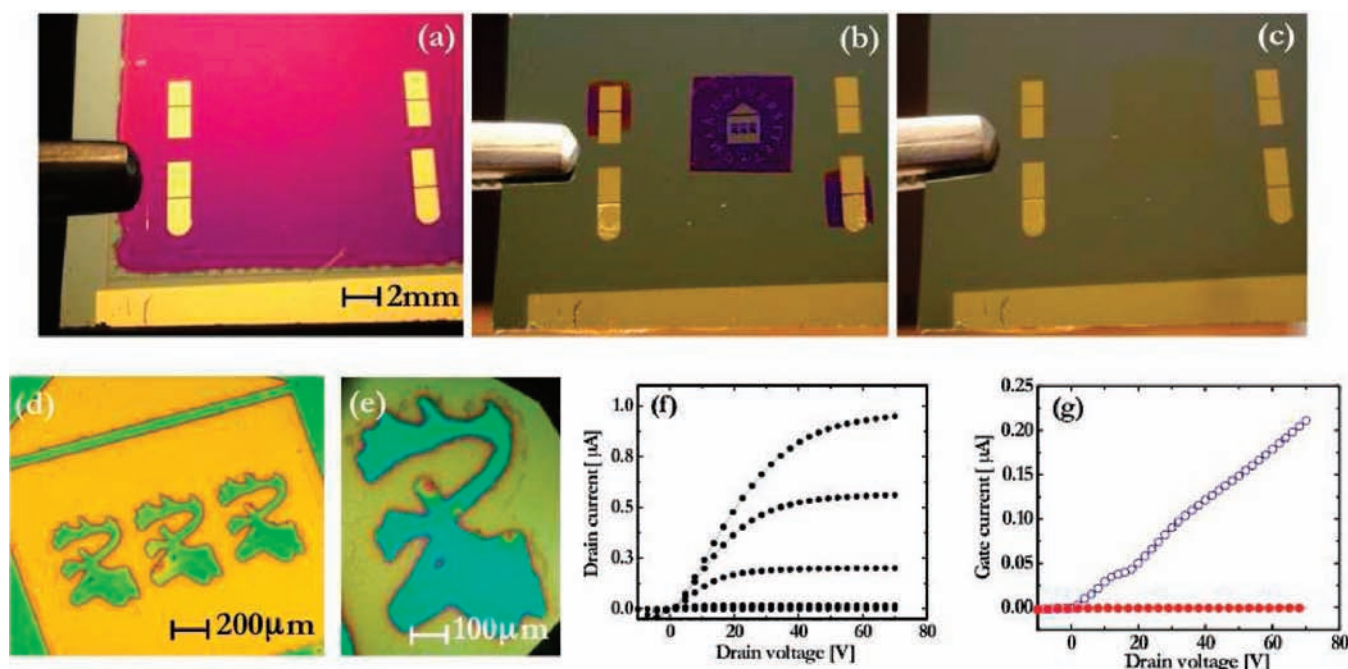


Figure 5. (a) Photograph of a spin-cast PCBM film deposited on a $\text{SiO}_2/\text{p-Si}$ substrate, on top of which four pairs of source-drain electrodes are fabricated. The electrode pairs define a 2×2 array of FETs. (b) Result of the PRI patterning process applied to the PCBM thin film. The employed mask for the exposure step defined two squares centered over two FET channels and a pattern comprising three reindeer heads. (c) Result of the subsequent development with a “strong” solvent that removed also the exposed PCBM material. (d) Magnification of the three reindeer heads. (e) Magnification of one reindeer head. (f) Output characteristics of a patterned-PCBM FET. (g) Comparison of the gate-leakage current in the same FET before (○) and after (■) the patterning process.

(indicative of very small contact resistances between the electrodes and the active material)³⁴ and a well-defined saturation of the drain current when the drain voltage exceeds the gate voltage.

The PRI patterning technique is also applicable to high-resolution patterning of optical-quality thin films. The PCBM

thin film in Figure 5a was fabricated by spin-casting, and Figure 5b, d, and e shows the end result of the PRI patterning at different magnification. We call specific attention to that fact

(34) Edman, L.; Swensen, J.; Moses, D.; Heeger, A. J. *Appl. Phys. Lett.* **2004**, *84*, 3744.

that is possible to pattern well-defined high-resolution features on the micrometer scale, as exemplified by the fact that the width of the eye of the reindeer in Figure 5e is less than $20\ \mu\text{m}$. The employed developer solution was a chloroform:acetone (1:3 by volume) mixture, and the development process is visualized in a movie. We find it appropriate to make the “good” solvent (i.e., chloroform) the minority component when thin spin-cast films are developed, but the majority component when thicker drop-cast films are developed. Furthermore, it is notable that it is possible to remove both the exposed (and dimerized) as well as the nonexposed portions of the PCBM film by development in a single-component chloroform solution, as visualized in Figure 5c.

Au source and drain electrodes were deposited on top of the PCBM film, which in turn was deposited on a $\text{SiO}_2/\text{p-Si}$ substrate. The Au electrodes defined a 2×2 array of FET structures (see Figure 5a). Figure 5f presents typical output characteristics for a patterned-PCBM FET (see Figure 5b), which exhibits well-behaved FET characteristics with a relatively high electron mobility ($\mu_n = 0.005\ \text{cm}^2/\text{Vs}$), a linear increase of the drain current in the linear regime, and a clear saturation in the saturation regime. The patterning of the PCBM film also brings the important advantage that the undesired gate-leakage currents can be minimized in an array of FETs. Figure 5g presents the measured gate leakage current in the same FET before (○) and after (■) the PCBM active material had been patterned (compare Figure 5a with b). The decrease in the overlap between the PCBM material outside the active FET channel and the gate electrode leads to a significant decrease of the gate leakage current of more than 1 order of magnitude.

The combined attractive features of the described PRI patterning technique open up for a range of applications, and we envision, for example, that high-speed printing of complex and easily adjusted transistor structures could be possible. One problem with current high-speed (gravure, flexo, offset, and screen) printing techniques is that they print the information that is stored on the printing roll, and that it consequently is

difficult to create large and complex structures and/or to easily adjust the initial pattern scheme. To resolve this problem, we suggest that a large array of transistors can be coated by a conventional offset printer, and that a computer-controlled high-power laser then exposes the active material in select transistors. Further down the line, the entire transistor array is washed with the developer solution, which removes the active material from the nonexposed transistors while leaving the function of the exposed transistors intact. One obvious commercial application of this technique is printed RFID tags, where programming each tag with a unique serial number often is desired.

IV. Conclusions

To conclude, we have demonstrated a gentle, simple and yet effective photoinduced and resist-free subtractive patterning method of solution-processed fullerene films for use in electronic devices. In the initial exposure step, select areas of a PCBM film are exposed to laser light, which chemically modifies the PCBM molecules from a monomeric to a dimeric structure and transforms them from being soluble to insoluble in a developer solution. In the final development step, the nonexposed areas of the film are removed by the developer solution while the exposed PCBM material is left intact. Importantly, the remaining patterned PCBM material retains a high electronic mobility, as evidenced by the fact that it is possible to fabricate optimized arrays of FETs comprising a patterned PCBM film as the active material.

Acknowledgment. We thank Dr. Nathaniel D. Robinson at Linköping University for valuable comments and Vetenskapsrådet for financial support. A.D. thanks Helge Ax:son Johnsons Foundation for support, and T.W. thanks Knut & Alice Wallenberg Foundation for support. L.E. is a “Royal Swedish Academy of Sciences Research Fellow” supported by a grant from the Knut and Alice Wallenberg Foundation.

JA807964X